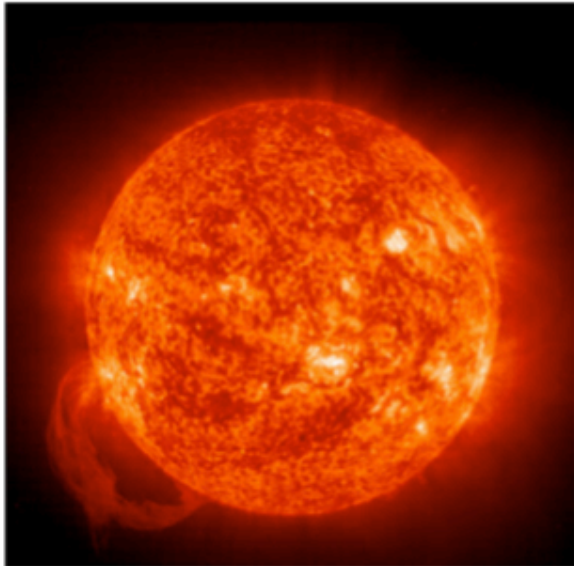
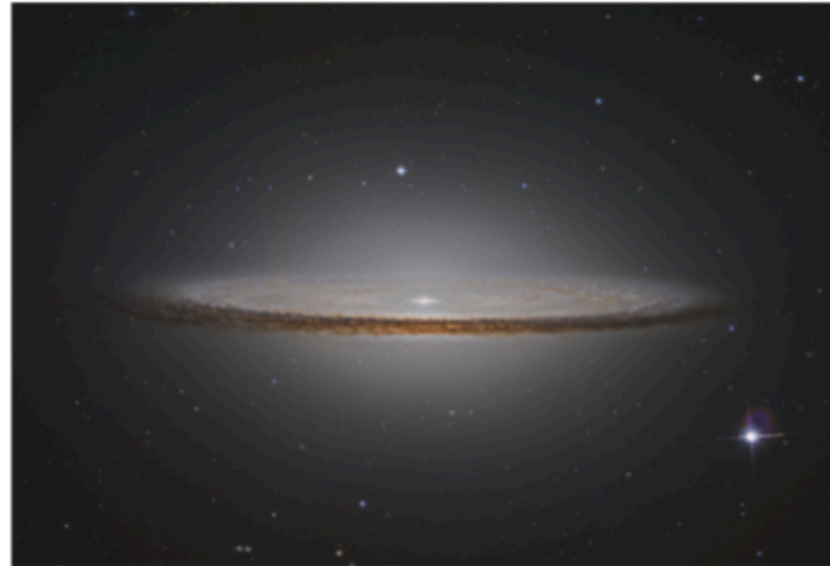


Pressure-supported

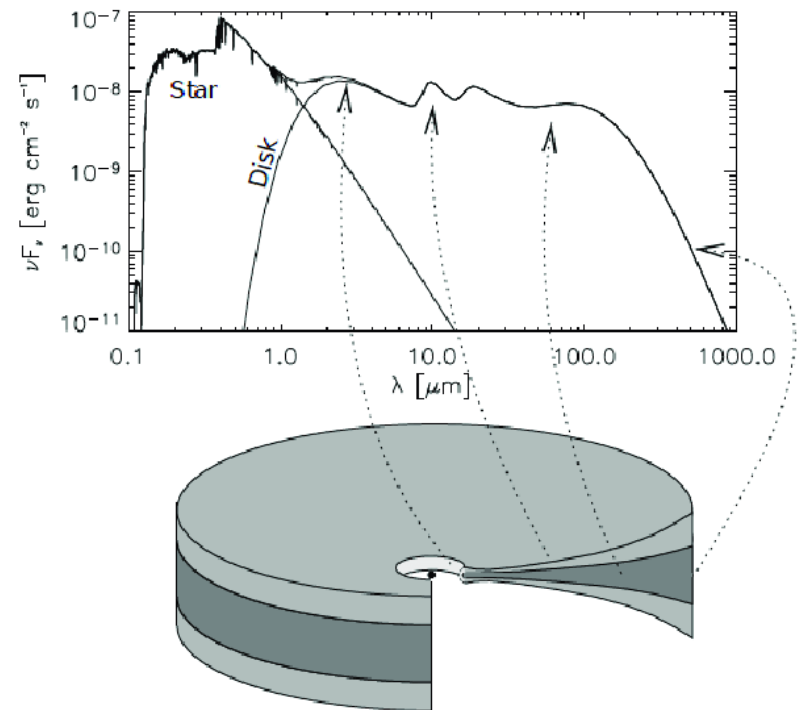
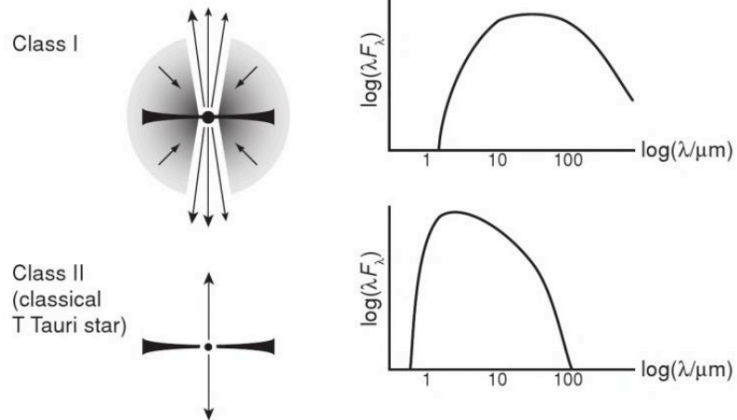


Rotation-supported



Angular Momentum

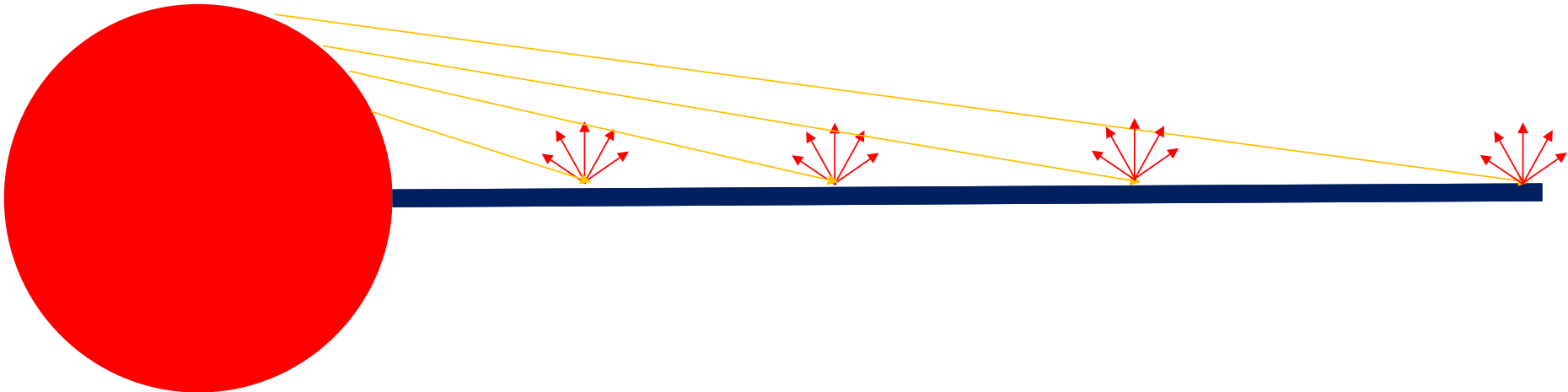
Class I and II differ by distribution of circumstellar matter



Flat disk



Flat disk



Flat disk



Disk Temperature Structure

THE ASTROPHYSICAL JOURNAL, 308: 836-853, 1986 September 15
© 1986. The American Astronomical Society. All rights reserved. Printed in U.S.A.

INFRARED SPECTRA OF ROTATING PROTOSTARS

FRED C. ADAMS AND FRANK H. SHU
Institute for Theoretical Physics
Received 1985 November 27; accepted 1986 March 4

ABSTRACT

We improve the numerical results of an earlier communication concerning the emergent spectral energy distribution expected for spherical protostars. Although this correction alleviates the problem of the missing mid-infrared radiation from the spherical models when they are compared with observations of actual protostellar candidates, the resulting spectra are still too steep, and the models tend to produce too much overall luminosity. In order to obtain better agreement with observations using more realistic assumptions, we generalize the technique to include the main effects of rotation. In our formulation, the radiation from an associated accretion disk is included explicitly, under the assumption that, in general, a fraction of the released gravitational energy can be stored as kinetic energy of differential rotation. Moreover, the treatment is exact for the absorption produced by the infalling dust envelope but only approximate for the dust emission by the use of a technique of an "equivalent spherical envelope." An exploration of parameter space reveals no surprises; in

THE ASTROPHYSICAL JOURNAL, 323: 714-733, 1987 December 15
© 1987. The American Astronomical Society. All rights reserved. Printed in U.S.A.

SPECTRAL ENERGY DISTRIBUTIONS OF T TAURI STARS: DISK FLARING AND LIMITS ON ACCRETION¹

S. J. KENYON² AND L. HARTMANN²
Harvard-Smithsonian Center for Astrophysics
Received 1987 April 13; accepted 1987 June 12

ABSTRACT

We analyze spectral energy distributions of T Tauri stars (TTS) to place limits on disk accretion in this early phase of stellar evolution. Our results reinforce the conclusion of Adams, Lada, and Shu that much of the infrared excess emission arises from reprocessing of stellar radiation by a dusty circumstellar disk. Although Adams, Lada, and Shu suggested that the flat infrared spectra of some objects might be indicative of a massive accretion disk, we show that a low-mass reprocessing disk can also produce relatively flat spectra if the disk flares slightly as radial distance increases. The amount of flaring required for many sources is physically plausible. However, it is difficult for the flared disk model to account for the relatively flat energy distributions, λF_λ is constant, exhibited by some TTS. Source confusion in long-wavelength observations and uncertainties in extinction corrections may help to explain the observed infrared energy distributions of these so-called flat-spectrum sources.

The strongest limits on accretion rates come from detection of possible boundary-layer radiation in the optical and near-ultraviolet regions. Boundary layer emission probably causes the strong optical continuum veiling seen in a few extremely active TTS. The relative importance of accretion and solar-type chromospheric activity is difficult to assess in most T Tauri stars, given the primitive nature of boundary layer and chromosphere models. Our analysis indicates that disk accretion in the T Tauri phase does not modify stellar evolution significantly and that the angular momentum of accreted material can be lost in a stellar wind.

Subject headings: spectrophotometry — stars: accretion — stars: flare — stars: mass loss — stars: pre-main-sequence

THE ASTROPHYSICAL JOURNAL, 490: 368-376, 1997 November 20
© 1997. The American Astronomical Society. All rights reserved. Printed in U.S.A.

SPECTRAL ENERGY DISTRIBUTIONS OF T TAURI STARS WITH PASSIVE CIRCUMSTELLAR DISKS

E. I. CHIANG AND P. GOLDREICH
California Institute of Technology, Pasadena, CA 91125; echiang@uftp.caltech.edu, pmg@nicholas.caltech.edu
Received 1997 March 18; accepted 1997 July 3

ABSTRACT

We derive hydrostatic, radiative equilibrium models for passive disks surrounding T Tauri stars. Each disk is encased by an optically thin layer of superheated dust grains. This layer reemits directly to space about half the stellar energy it absorbs. The other half is emitted inward and regulates the interior temperature of the disk. The heated disk flares. As a consequence, it absorbs more stellar radiation, especially at large radii, than a flat disk would. The portion of the spectral energy distribution contributed by the disk is fairly flat throughout the thermal infrared. At fixed frequency, the contribution from the surface layer exceeds that from the interior by about a factor 3 and is emitted at more than an order of magnitude greater radius. Spectral features from dust grains in the superheated layer appear in emission if the disk is viewed nearly face-on.

Subject headings: accretion, accretion disks — circumstellar matter — infrared: stars — radiative transfer — stars: pre-main-sequence

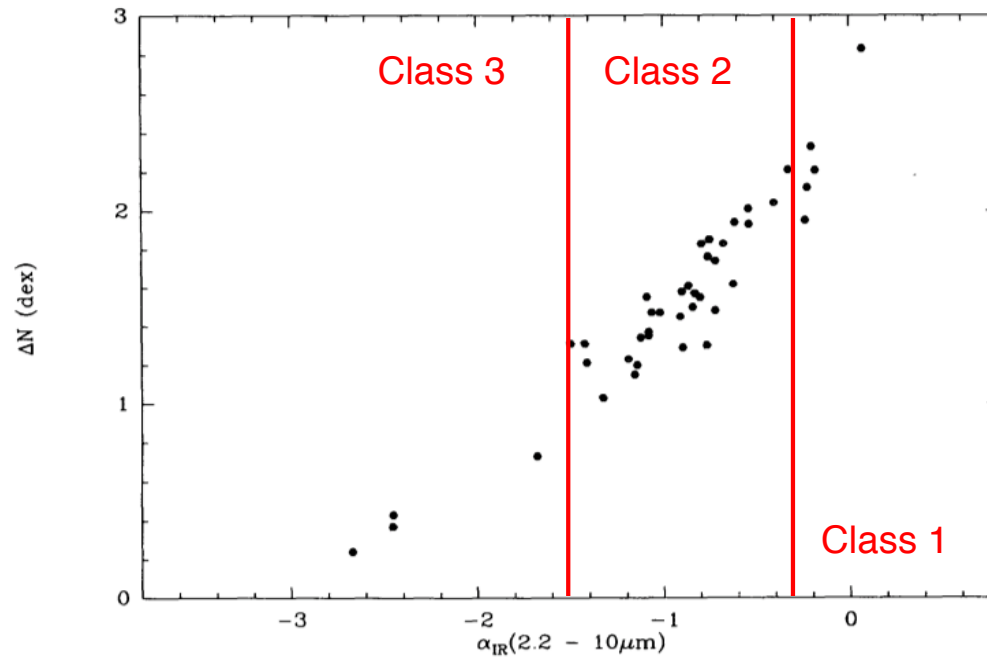


FIG. 2.—Plot of the 10 μm IR excess ΔN vs. the near-IR spectral index α_{IR} measured between 2.2 and 10 μm , for the T Tauri stars of Taurus-Auriga. The good correlation suggests that α_{IR} may be used as an indicator of the 10 μm excess for highly extinguished stars where it is difficult to measure directly by comparison with the photosphere. $\Delta N \sim 1$ marks the boundary between optically thin and optically thick disk emission at 10 μm (cf. Skrutskie et al. 1990).

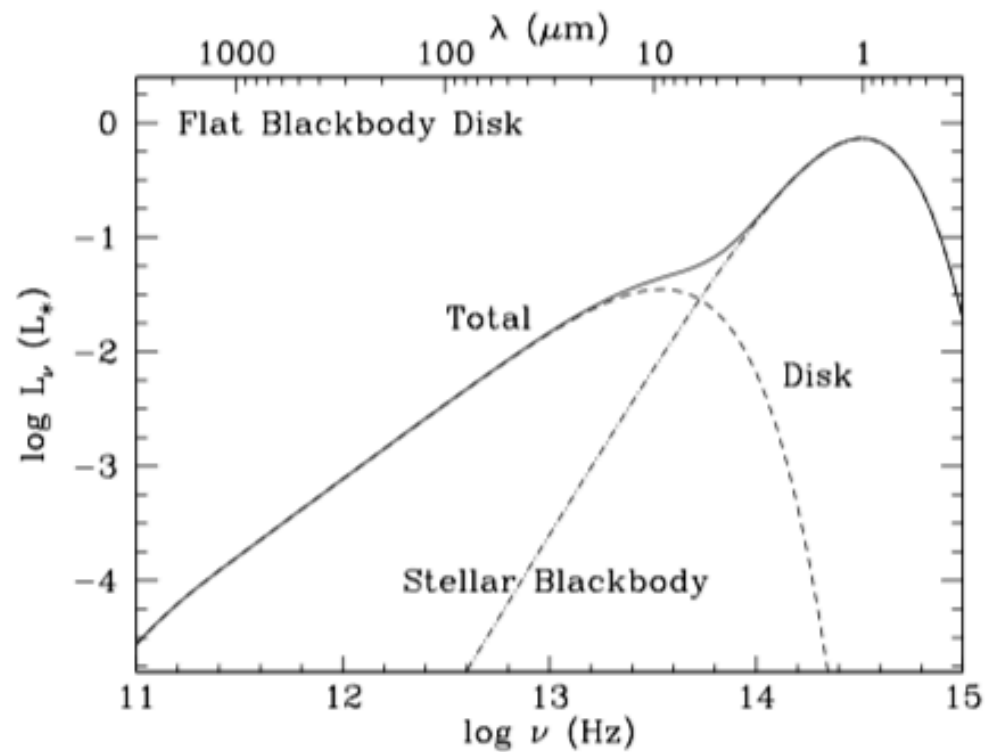


FIG. 1.—SED for the flat blackbody disk, with contributions from star and disk identified. The $n = 4/3$ law is evident between $30\ \mu\text{m}$ and $1\ \text{mm}$. The turnover near $1\ \text{mm}$ is due to our truncation of the disk at $a_o \approx 270\ \text{AU}$.

The long way (Adams & Shu 1986)

APPENDIX HEATING AND SHADOWING

Consider the mutual heating and shadowing of two elements of area, dA_* with unit normal \hat{r} on the surface of the star and dA_D with unit normal \hat{z} on the surface of the disk. For purposes of integration over the star when dA_D is held fixed, let the vector position of dA_* expressed in spherical polar coordinates be $\mathbf{r}_* = (R_*, \theta, \phi)$, and let the vector position of dA_D be $\mathbf{r}_D = (r_D, \pi/2, 0)$. (We assume here that the disk is perfectly thin and flat; the effects are larger if the disk flares outward or is warped.) For integration over the disk when dA_* is held fixed, it is preferable to ascribe the azimuthal coordinate ϕ to the disk. A light ray from \mathbf{r}_* to \mathbf{r}_D has the path vector,

$$\mathbf{s} = \mathbf{r}_D - \mathbf{r}_*, \quad (\text{A1})$$

where s is the path length,

$$s = (R_*^2 + r_D^2 - 2R_*r_D \sin \theta \cos \phi)^{1/2}, \quad (\text{A2})$$

and \mathbf{n} is the unit propagation vector with the direction cosines,

$$\mathbf{n} \cdot \hat{r} = \frac{1}{s} (\mathbf{r}_D - \mathbf{r}_*) \cdot \hat{r} = \frac{1}{s} (r_D \sin \theta \cos \phi - R_*), \quad (\text{A3a})$$

$$\mathbf{n} \cdot \hat{z} = \frac{1}{s} (\mathbf{r}_D - \mathbf{r}_*) \cdot \hat{z} = -\frac{R_*}{s} \cos \theta. \quad (\text{A3b})$$

If we assume that the disk lies within the opacity gap so that no absorption occurs, the rate, $d\dot{E}_*$, at which radiant energy of frequency ν traveling from dA_* is intercepted by dA_D equals

$$d\dot{E}_* = I_\nu(\mathbf{n} \cdot \hat{r}) dA_* (-\mathbf{n} \cdot \hat{z}) dA_D / s^2. \quad (\text{A4})$$

We assume that I_ν can be approximated as a Planck function $B_\nu(T(\theta))$. Integrated over all frequencies and the part of the surface area of the star which can be seen by dA_D , the upper face of the disk at θ intercepts, per unit area and time, the amount of energy:

$$\frac{d\dot{E}_*}{dA_D} = \frac{1}{\pi} \int_{\theta_*}^{\pi/2} \sigma T_*^4(\theta) \sin \theta \cos \theta d\theta \int_{-\phi_*}^{+\phi_*} \left(\frac{R_*}{s} \right)^4 \left(\frac{r_D}{R_*} \sin \theta \cos \phi - 1 \right) d\phi. \quad (\text{A5})$$

For given θ , the range of the ϕ integration is confined to angles between where $\mathbf{n} \cdot \hat{r} = 0$, i.e., from $-\phi_*$ to $+\phi_*$ where

$$\cos \phi_* = R_*/r_D \sin \theta. \quad (\text{A6})$$

The contribution closest to the pole of the star originates at $\theta = \theta_*$ with

$$\sin \theta_* = R_*/r_D. \quad (\text{A7})$$

so that $\phi_* = 0$ at this point.

In a steady state, the upper (and lower) side of the disk must radiate not only its own accretion energy, but also the intercepted stellar radiation,

$$\sigma T_D^4(\pi) = \left[\frac{L_D}{4\pi R_*^2 (1 - R_*/R_D)} \right] \left(\frac{r_D}{R_*} \right)^{-3} + \frac{d\dot{E}_*}{dA_*}, \quad (\text{A8})$$

where L_D is given by equation (33b). In a similar fashion, the star must radiate not only its accretion energy, but also the intercepted disk radiation,

$$\sigma T_*^4(\theta) = \frac{1}{2} \rho |v_r|^3 + \eta_* [1 - (1 - \eta_D) \mathcal{H}_D] [1 - (1 - \eta_D)(1 - u_*^{1/2})] \frac{L_D}{8\pi R_*^2} + \frac{d\dot{E}_D}{dA_*}, \quad (\text{A9})$$

where $\rho |v_r|^3 / 2$ is the rate of release of impact energy by direct infall and where we have spread the stellar dissipation of rotational energy in a spherically symmetric manner for lack of better knowledge. In equation (A9), the rate of intercepted disk energy is

$$\frac{d\dot{E}_D}{dA_*} = \frac{1}{\pi} \cos \theta \int_{\theta_*}^{\pi/2} \sigma T_D^4(\pi) \frac{r_D d\pi}{R_*^2} \int_{-\phi_*}^{+\phi_*} \left(\frac{R_*}{s} \right)^4 \left(\frac{r_D}{R_*} \sin \theta \cos \phi - 1 \right) d\phi, \quad (\text{A10})$$

where

$$\theta_* = R_*/r_D \sin \theta, \quad (\text{A11})$$

is the smallest radius of the disk observable at θ on the star.

In principle, equations (A8) and (A9) should also include the effect of the back warming of a hot dust envelope (see SST 1980 for a discussion of this effect in the nonrotating context). If the infalling envelope is optically thick near the dust destruction front, heating by the infalling dust envelope effectively adds the terms $\gamma_*(\pi)\sigma T_*^4$ and $\gamma_D(\theta)\sigma T_D^4$, respectively, to the right-hand sides of equations

(A8) and (A9), where $\gamma_*(\pi)$ is the fraction of the sky viewed from π in the disk not blocked by the star and $\gamma_D(\theta)$ is the fraction of the sky viewed from θ on the star not blocked by the disk. In practice, as long as T_*^4 and T_D^4 remain large in comparison with T_r^4 , this correction is a minor effect.

Equations (A8) and (A9), together with the subsidiary definitions (A5) and (A10), constitute two coupled integral equations which determine $T_D(\pi)$ and $T_*(\theta)$. For the purposes of this Appendix, it suffices to find an approximate global solution to the set. We assume $T_*(\theta) = \text{constant} \equiv T_*$ and $T_D(\pi) = T_D(\pi/R_*)^{-3/4}$, and we choose the constants T_* and T_D so that equations (A8) and (A9) are valid when integrated over the entire surfaces of disk and star. The integrations with respect to dA_D and dA_* produce two requirements:

$$4\pi R_*^2 \left(1 - \frac{R_*}{R_D} \right) \sigma T_D^4 = L_D + \dot{E}_*, \quad (\text{A12a})$$

$$4\pi R_*^2 \sigma T_*^4 = L_* + \dot{E}_D, \quad (\text{A12b})$$

where L_* is given by equation (33a) and

$$\dot{E}_* = 8R_*^2 \sigma T_*^4 \int_{R_*}^{R_D} \frac{r_D dr_D}{R_*^2} \int_{\theta_*}^{\pi/2} \sin \theta \cos \theta d\theta \int_0^{2\pi} \left(\frac{R_*}{s} \right)^4 \left(\frac{r_D}{R_*} \sin \theta \cos \phi - 1 \right) d\phi, \quad (\text{A13a})$$

$$\dot{E}_D = 8R_*^2 \sigma T_D^4 \int_{\theta_*}^{\pi/2} \sin \theta \cos \theta d\theta \int_{\theta_*}^{R_D} \left(\frac{r_D}{R_*} \right)^{-3} \frac{r_D dr_D}{R_*^2} \int_0^{2\pi} \left(\frac{R_*}{s} \right)^4 \left(\frac{r_D}{R_*} \sin \theta \cos \phi - 1 \right) d\phi, \quad (\text{A13b})$$

with

$$\sin \theta_* = R_*/R_D. \quad (\text{A14})$$

We can write equations (A13a) and (A13b) in the suggestive forms:

$$\dot{E}_* = f_D 4\pi R_*^2 \left(1 - \frac{R_*}{R_D} \right) \sigma T_*^4, \quad (\text{A15a})$$

$$\dot{E}_D = f_* 4\pi R_*^2 \sigma T_D^4, \quad (\text{A15b})$$

where by introducing the transformation of variables:

$$u \equiv R_*/r_D, \quad v \equiv \sin \theta, \quad w \equiv \cos \phi,$$

and by switching one order of integration, we may express f_D and f_* as the dimensionless integrals:

$$f_D = \frac{2}{\pi(1 - u_{*D})} \int_{u_{*D}}^1 h(u) du, \quad f_* = \frac{2}{\pi} \int_{u_{*D}}^1 u^3 h(u) du, \quad (\text{A16a})$$

$$h(u) \equiv \int_0^1 v dv \int_{v_*}^1 \frac{(vw - u) dw}{(1 - w^2)^{1/2} (1 + u^2 - 2uvw)^2}, \quad (\text{A16b})$$

with $u_{*D} = R_*/R_D$. By a judicious change of variables (motivated by switching to a spherical coordinate system the line joining the center of the star and the disk point is the polar axis), we can integrate equation (A16b) to get

$$h(u) = \frac{1}{2u^2} [\arcsin u - u(1 - u^2)^{1/2}]. \quad (\text{A17})$$

The substitution of equation (A17) into equations (A16a) now yields

$$f_D = \frac{1}{(1 - u_{*D})} \left[\frac{1}{4} - \frac{1}{\pi} \left(1 - \frac{1}{2u_{*D}^2} \right) \arcsin u_{*D} - \frac{1}{2\pi u_{*D}} (1 - u_{*D}^2)^{1/2} \right], \quad (\text{A18a})$$

$$f_* = \frac{1}{2} - \frac{u_{*D}}{\pi} \arcsin u_{*D} - \frac{1}{3\pi} (1 - u_{*D}^2)^{1/2} (4 - u_{*D}^2). \quad (\text{A18b})$$

The functions f_D and f_* are tabulated in Table 3; of special interest are the limiting values, $f_D = 1/4$ and $f_* = 1/2 - 4/3\pi = 0.0756$ for $u_{*D} = 0$. Note also that $f_D = 1/2$ for $u_{*D} = 1$ because half of the sky is filled by the stellar surface for a narrow disk at the equator of the star.

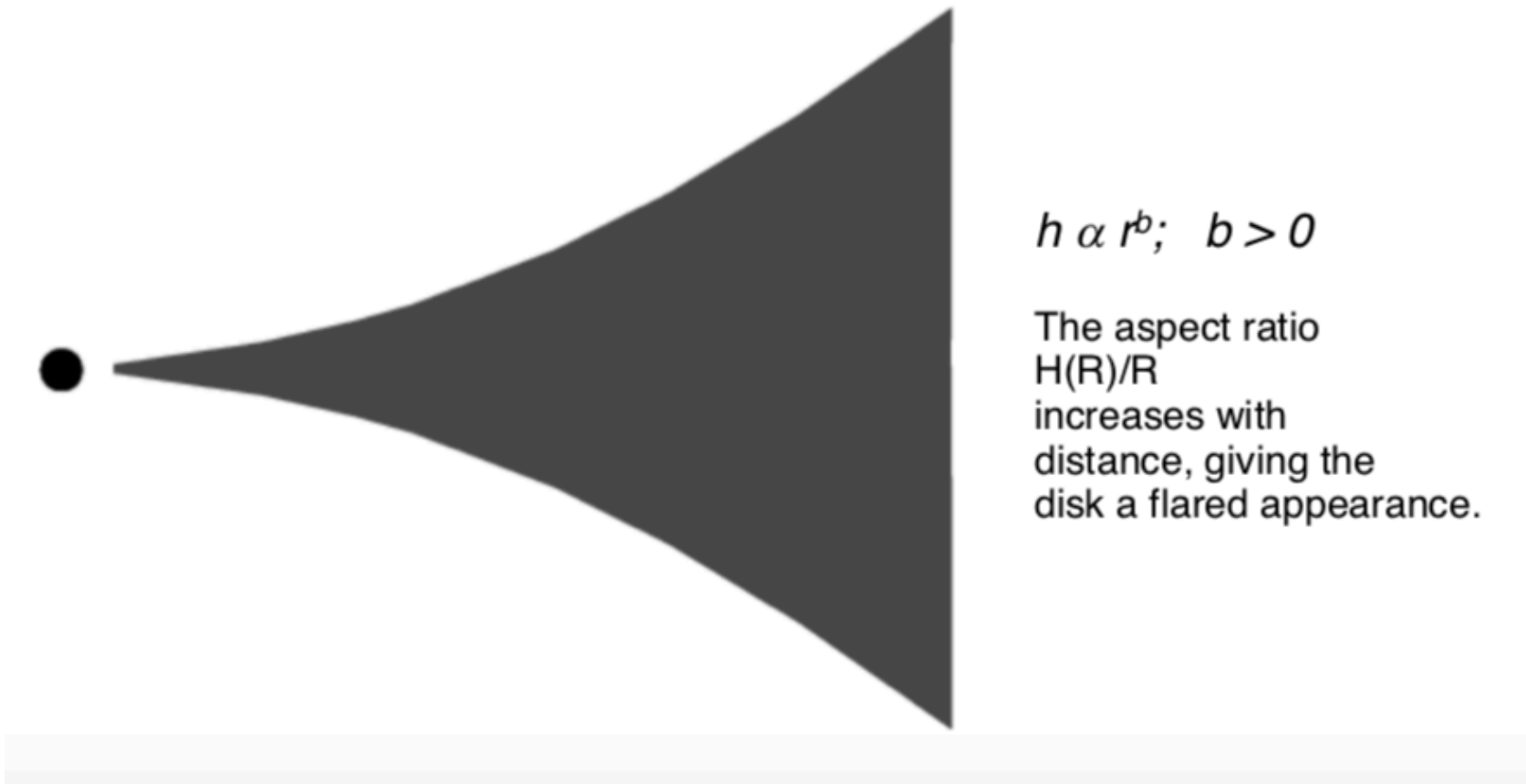
With equations (A15a) and (A15b) giving \dot{E}_* and \dot{E}_D , we may solve equations (A12a) and (A12b) as a set of simultaneous linear equations for σT_*^4 and σT_D^4 , obtaining

$$\sigma T_*^4 = \frac{1}{(1 - f_* f_D)} \left[\frac{L_*}{4\pi R_*^2} + f_* \frac{L_D}{4\pi R_*^2 (1 - u_{*D})} \right], \quad (\text{A19a})$$

$$\sigma T_D^4 = \frac{1}{(1 - f_* f_D)} \left[\frac{L_D}{4\pi R_*^2 (1 - u_{*D})} + f_D \frac{L_*}{4\pi R_*^2} \right]. \quad (\text{A19b})$$

Vertical structure: Hydrostatic Equilibrium

Disks are “flared”



SPECTRAL ENERGY DISTRIBUTIONS OF T TAURI STARS: DISK FLARING AND LIMITS ON ACCRETION¹

S. J. KENYON² AND L. HARTMANN²
 Harvard-Smithsonian Center for Astrophysics
 Received 1987 April 13; accepted 1987 June 12

ABSTRACT

We analyze spectral energy distributions of T Tauri stars (TTS) to place limits on disk accretion in this early phase of stellar evolution. Our results reinforce the conclusion of Adams, Lada, and Shu that much of the infrared excess emission arises from reprocessing of stellar radiation by a dusty circumstellar disk. Although Adams, Lada, and Shu suggested that the flat infrared spectra of some objects might be indicative of a massive accretion disk, we show that a low-mass reprocessing disk can also produce relatively flat spectra if the disk flares slightly as radial distance increases. The amount of flaring required for many sources is physically plausible. However, it is difficult for the flared disk model to account for the relatively flat energy distributions, $\lambda F_\lambda \approx \text{constant}$, exhibited by some TTS. Source confusion in long-wavelength observations and uncertainties in extinction corrections may help to explain the observed infrared energy distributions of these so-called flat-spectrum sources.

The strongest limits on accretion rates come from detection of possible boundary-layer radiation in the optical and near-ultraviolet regions. Boundary layer emission probably causes the strong optical continuum veiling seen in a few extremely active TTS. The relative importance of accretion and solar-type chromospheric activity is difficult to assess in most T Tauri stars, given the primitive nature of boundary layer and chromosphere models. Our analysis indicates that disk accretion in the T Tauri phase does not modify stellar evolution significantly and that the angular momentum of accreted material can be lost in a stellar wind.

Subject headings: spectrophotometry — stars: accretion — stars: flare — stars: mass loss — stars: pre-main-sequence

b) Plausibility of Flared Disks

The considerations of the preceding paragraphs motivated us to examine modifications of reprocessing disk models. An optically thick disk with a concave upper surface will intercept a larger percentage of the stellar radiation than a completely flat disk. Disks will tend to “flare” in this fashion for the following reason. In a system where the central star contains essentially all of the mass, the scale height, h , varies with radius, R , as (SS):

$$\frac{h}{R} = \left(\frac{v_s^2 R}{GM_*} \right)^{1/2}, \quad (1)$$

where G is the gravitational constant, M_* is the stellar mass, and v_s is the sound speed. Thus, if $T_{\text{int}}(R) \propto v_s^2$ falls off more slowly than R^{-1} , then the relative thickness of the disk will increase outward. For an internal temperature distribution, $T_{\text{int}}(R)$, similar to the flat disk *surface* temperature distribution $T_d \propto R^{-3/4}$, $h/R \propto R^{1/8}$, and the disk curvature will become more important at increasing radial distances. Outer regions of the disk then receive more radiation from the central star, so the IR spectrum from a flared disk will fall off less steeply with increasing wavelength than the spectrum of a flat disk.

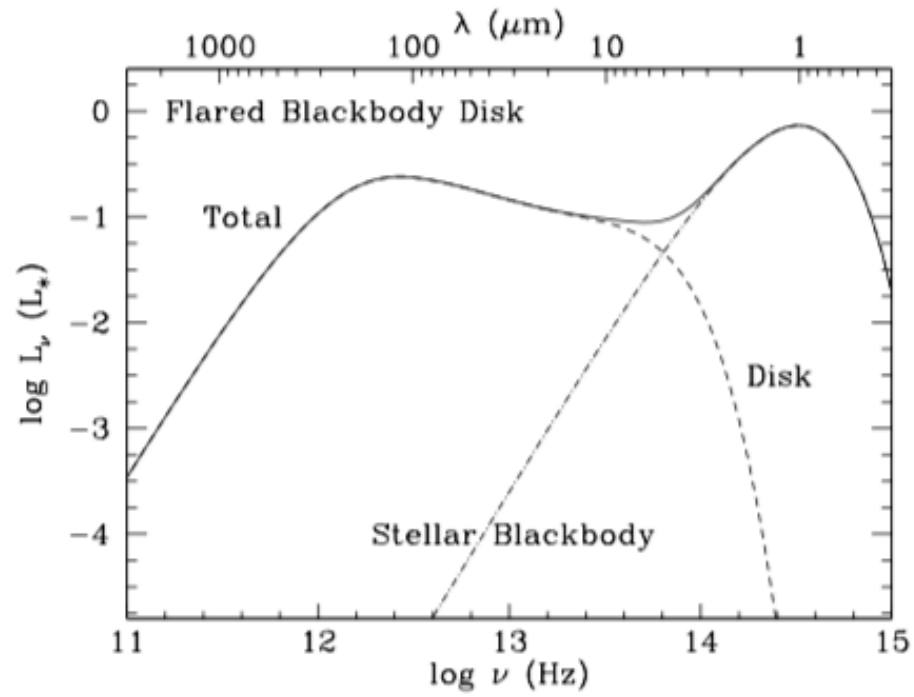


FIG. 2.—SED for the flared blackbody disk. At mid-IR wavelengths, $L_\nu \propto \nu^{-2/3}$. At longer wavelengths, $L_\nu \propto \nu^3$.

